LANGMUIR Article
Cite This: Langmuir 2019, 35, 921−927
pubs.acs.org/Langmuir

How To Obtain Six Different Superwettabilities on a Same Microstructured Pattern: Relationship between Various Superwettabilities in Different Solid/Liquid/Gas Systems

Jiale Yong,[†,‡] Subhash C. Singh,[†] Zhibing Zhan,[†] Feng Chen,*[,‡] and Chunlei Guo*[,†]

[†]The Institute of Optics, University of Rochester, Rochester, New York 14627, United States
[‡]Shaanxi Key Laboratory of Photonics Technology for Information, School of Electronics & Information Engineering, Xi'an Jiaotong University, Xi'an, 710049, People's Republic of China

Supporting Information

ABSTRACT: A range of different superwettabilities were obtained on femtosecond laser-structured Al surfaces. The formation mechanism of each superwetting state is discussed in this paper. It is revealed that the underwater oil droplet and bubble wettabilities of a solid surface have a close relationship with its water wettability. The laser-induced hierarchical microstructures showed superhydrophilicity in air but showed superoleophobicity/superaerophobicity after immersion in water. When such microstructures were further modified with a low-surface-energy monolayer, the wettability of the resultant surface would turn to superhydrophobicity with ultralow water adhesion in air and superoleophilicity/superaerophilicity in water. The understanding of the relationship among the above-mentioned six different superwettabilities is highly important in the design of various superwetting microstructures, transforming the structures from one superwetting state to another state and better using the artificial superwetting materials.

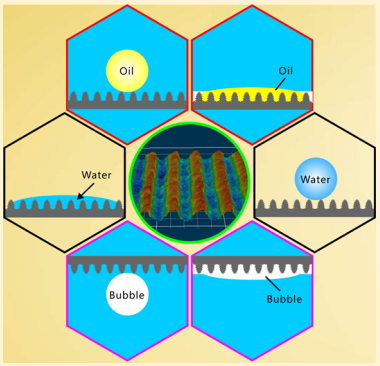

INTRODUCTION

There are three common states of matter in our daily life, i.e., solid, liquid, and gas. They often coexist, forming different solid/liquid/gas interfaces. Among them, the different wettabilities at the solid/liquid/gas interfaces have rich practical applications, e.g., liquid repellence,[1] small droplet manipulation,[2−4] self-cleaning materials,[5,6] oil/water separation,[7−9] anti-icing,[10] microfluidics,[11,12] cell engineering,[13−15] fog harvest,[16] and underwater gas collection.[17,18] In nature, the surface of the lotus leaf has excellent superhydrophobicity, which allows water droplets to easily roll off the lotus leaf and take contaminations away.[19] The great water repellency and the self-cleaning function of the lotus leaf are caused by the collective effects of the binary microstructures (including the microscale papillae and the nanoscale branches) and the hydrophobic wax-crystal coating on its surface.[20−22] In addition, fish skin resists oil contamination because the fish scales show underwater superoleophobicity that endow fish scales with great anti-oil ability in water.[23] It is found that a lot of oriented micropapillae with fine nanoscale pimples are distributed on the fish scales.[23,24] Recently, we demonstrated that lotus leaves also show underwater superaerophilicity and can capture bubbles in water, while fish scales exhibit underwater superaerophobicity and have the ability to prevent the bubbles from adhering to fish skin.[22] Inspired by nature, researchers have produced various kinds of superwettabilities, including superhydrophilicity/phobicity, underwater superoleophilicity/phobicity, and underwater superaerophilicity/phobicity.[25−31] One or two kinds of these superwettabilities are usually obtained on a solid surface by the formation of proper microstructures. However, achieving the superhydrophilicity, superhydrophobicity, underwater superoleophilicity, underwater superoleophobicity, underwater superaerophilicity, and underwater superaerophobicity on the same microstructured pattern still remains a challenge. The relationship between the above-mentioned different superwettabilities should be clearly revealed, which is important in the design of different superwetting microstructures, the interconversion between different superwettabilities, and better application of the artificial superwetting materials.

In this paper, a hierarchical microstructured pattern was simply created on an Al surface via femtosecond (fs) laser pulses. The original laser-structured surface was superhydrophilic in air and had superoleophobicity/aerophobicity in water. When the surface was further modified with fluoroalkylsilane, its wettability was transformed to in-air superhydrophobicity and underwater superoleophilicity/aerophilicity. Therefore, six kinds of different superwetting states were obtained on the laser-induced microstructures. The formation mechanisms of these superwettabilities were discussed individually. Furthermore, the relationship between different superwettabilities was revealed.

Received: November 5, 2018
Revised: December 4, 2018
Published: January 4, 2019

DOI: 10.1021/acs.langmuir.8b03726
Langmuir 2019, 35, 921−927

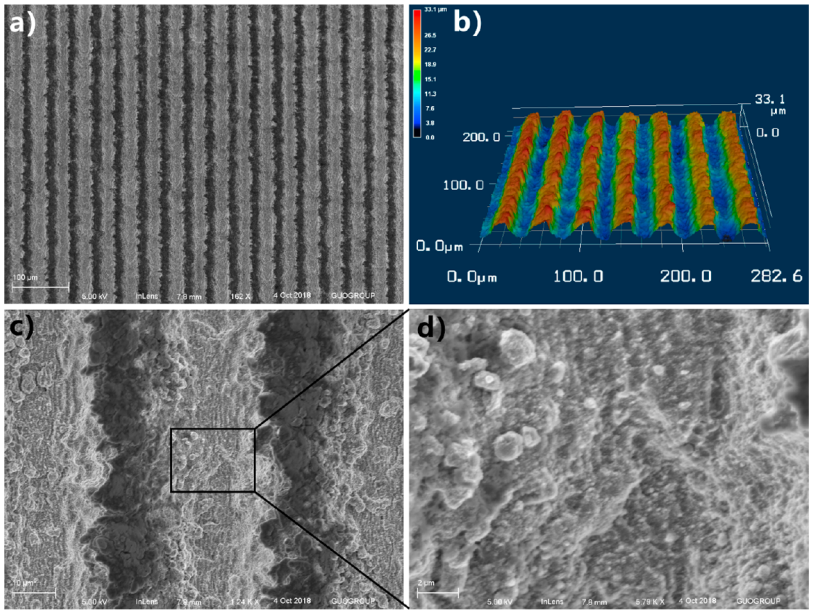

Figure 1. SEM images and 3D profile of the laser-structured Al surface. (a) SEM image and (b) laser confocal microscopy image of the microgrooves array. (c) Ridges between the microgrooves. (d) SEM image of the top surface of the ridge.

EXPERIMENTAL SECTION

Fabrication of Surface Microstructure. The method of fs laser ablation was employed to creating a surface microstructure on an Al sheet. With the use of a plano-convex lens (focal length = 250 mm) the laser beam (wavelength = 800 nm, pulse width = 67 fs, repetition rate = 1000 Hz) was focused on the surface of the Al sheet that was mounted on a translation stage in advance. The Al surface was ablated by the laser at the power of 200 mW, the space of the scanning lines of 40 μm, and the scanning speed of 2 mm/s, respectively. The laser-ablated surface was finally cleaned with alcohol and distilled water in an ultrasonic cleaner. In this paper, the original laser-structured Al surface is defined as the "rough surface".

Reduction of the Surface Free Energy. To reduce the surface free energy of the laser-ablated Al substrate, the common fluoroalkylsilane modification was used in this experiment. After laser treatment, the cleaned sample was dipped into a 1% alcohol solution of fluoroalkylsilane (1H,1H,2H,2H-perfluorodecyltriethoxysilane) for 1 day. The sample surface was then lightly rinsed with ethanol to remove the excess fluoroalkylsilane molecules. Next, the Al sheet was stored at 100 °C for 1 h, making the grafted fluoroalkylsilane monolayer more stable. The fluoroalkylsilane-modified rough surface is defined as the "F-rough surface" in this paper.

Characterization. The laser-induced structure was measured by an S-4100 scanning electron microscope (SEM, Hitachi, Japan), and the corresponding three-dimensional (3D) profile was obtained by a VK-9700 laser confocal microscope (Keyence, Japan). The wettabilities of the water droplet and the underwater oil droplet/bubble on the as-prepared surfaces were investigated by a SL2000KB contact-angle measurement (Kino, America), including the contact angle (CA) and sliding angle (SA). The distilled water, chloroform, and air were adopted as the detecting water, oil, and bubble, respectively. The dynamic processes related to wettability were captured by a camera at 25 frames per second.

RESULTS AND DISCUSSION

Laser-Induced Microstructure. Figure 1a,c,d includes the SEM images of the laser-ablated Al surface. Every laser scanning line could turn to a single groove, thereby an array of grooves was fabricated by line-by-line scanning (Figure 1a). The depth of the grooves is ~20.9 μm and the width is ~35.2 μm (Figure 1b). The microgrooves are arranged periodically, whose period (40 μm in this experiment) is controlled by the space of the laser scanning lines. The ridges are formed between the microgrooves. There are abundant nanoparticles randomly decorating the surface of every ridge that form a kind of micro/nanoscale hierarchical structure (Figure 1cd). The deep microgrooves were mainly caused by the laser-induced material removal, while the nanoparticles resulted from the resolidification of the ejected particles during laser ablation.[32,33] The used laser intensity in this experiment is very high and distributes as Gauss curve. The fluence at the spot center is the highest, resulting in a strong ablation at the laser-focused point. The irradiated materials on the Al surface are heavily removed away, so microgrooves are generated in the center of the laser scanning lines. During laser ablation, the material near the spot center is removed and sputtered above the Al substrate in the form of nanoscale molten particles. As such, the ejected particles fall back toward the Al surface and resolidify; abundant nanoparticles are formed on the surface of the microgrooves. As a result, a hierarchical microstructure was directly obtained by a one-step femtosecond laser treatment. Because the microgrooves are an inherent part of the Al substrate and the nanoparticles are recast onto the microgrooves, the femtosecond laser-induced microstructure is very stable.

Water Wettability. The water wettability of the laser-structured rough and F-rough surfaces was investigated by placing a water droplet on the sample surfaces. The original laser-ablated surface shows superhydrophilicity in air (Figure 2a). The water spread out quickly on the rough surface once the water droplet touched the laser-treated area (Figure 3a and Movie S1 in the Supporting Information). Finally, the water CA (WCA) was only 1.7 ± 1.8°. Previously, the enhancement function of the hydrophilicity of the different solid substrates by the femtosecond laser-induced surface microstructures was already demonstrated.[34−37] The wetting state of the water droplet on the microstructure belongs to the Wenzel model (Figure 2c).[1] The water is able to fully wet the substrate; that

DOI: 10.1021/acs.langmuir.8b03726
Langmuir 2019, 35, 921−927

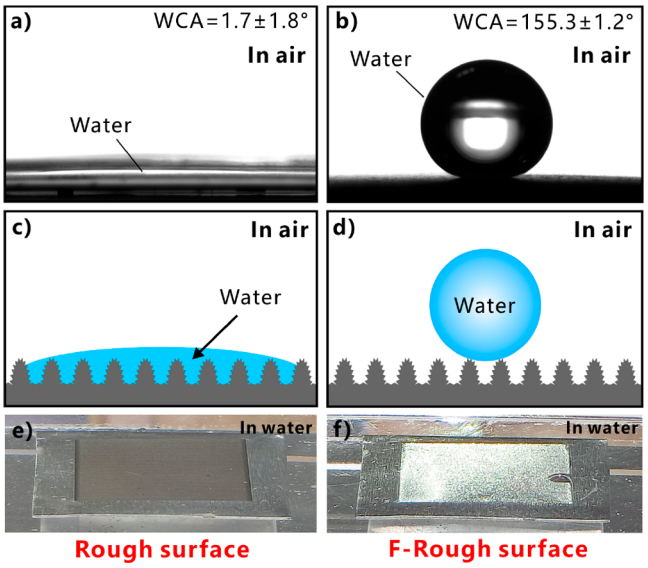

Figure 2. Water wettabilities of the as-prepared rough and the F-rough surfaces, respectively. (a, b) Images of a water droplet on the as-prepared surfaces: (a) the rough surface and (b) the F-rough surface. (c, d) Wetting states of a water droplet on the rough and the F-rough substrates: (c) Wenzel state and (d) Cassie state. (e, f) Photographs of the as-prepared samples in water: (e) the rough surface and (f) the F-rough surface.

is, water can penetrate into the valley of the hierarchical microstructures, because of the inherent hydrophilicity of the Al material and the amplification effect of the rough microstructures toward surface wettability. Regarding the F-rough surface that was treated by laser and fluoroalkylsilane, the water droplet maintained a spherical shape on such a surface with a WCA of 155.3 ± 1.2° (Figure 2b). This droplet rolled off as the sample was tilted to 6.3 ± 1.2° (Figure 3d and Movie S2 in the Supporting Information). Therefore, the F-rough surface exhibits superhydrophobicity and ultralow adhesion to water droplets. Similar ultralow adhesive superhydrophobicity can also be achieved on various inherently hydrophilic or hydrophobic materials by simple femtosecond laser treatment.[4,21,32,33,38−42] The cooperation between the laser-induced roughness and the low-surface-energy fluoroalkylsilane monolayer effectively inhibits the contact between the water droplet and the microstructure of the F-rough surface. The water droplet is at the Cassie contact state (Figure 2d).[1] The water droplet looks like it is being lifted by the hierarchical microstructures and touches just the top part of the microstructures. So a small contact area between the microstructure and the water droplet leads to the superhydrophobicity of the F-rough surface. The Cassie wetting state can be confirmed by dipping the sample into water. It was found that a silver-mirror reflectance appeared around the textured area, which demonstrated the existence of a gas layer between the water and the substrate (Figure 2f).[43,44] In contrast, the mirror-like reflectance was not found after the immersion of an original rough surface in water (Figure 2e).

Underwater Oil Wettability. If the laser-induced superhydrophilic rough surface was immersed in water, the surface would have an excellent oil-repellent function. The underwater oil (chloroform) droplet on the surface had an oil CA (OCA) of 155.1 ± 1.4° (Figure 4a) and freely rolled away at a 1.9 ± 1.4° tilted surface (Figure 3b and Movie S3 in the Supporting Information), revealing that the hierarchical microstructure had superoleophobicity and extremely low oil-adhesion underwater. Such laser-induced underwater superoleophobicity is the same as Wu's result.[45] The formation of the ultralow oil-adhesive superoleophobicity (in water) of the rough surface microstructure has a close relationship with its superhydrophilicity (in air). The microstructure is completely wetted by water in a water medium (Figure 4c). After further placing an oil droplet onto the surface, a water cushion forms between the oil and the substrate (Figure 4e). The cushion is

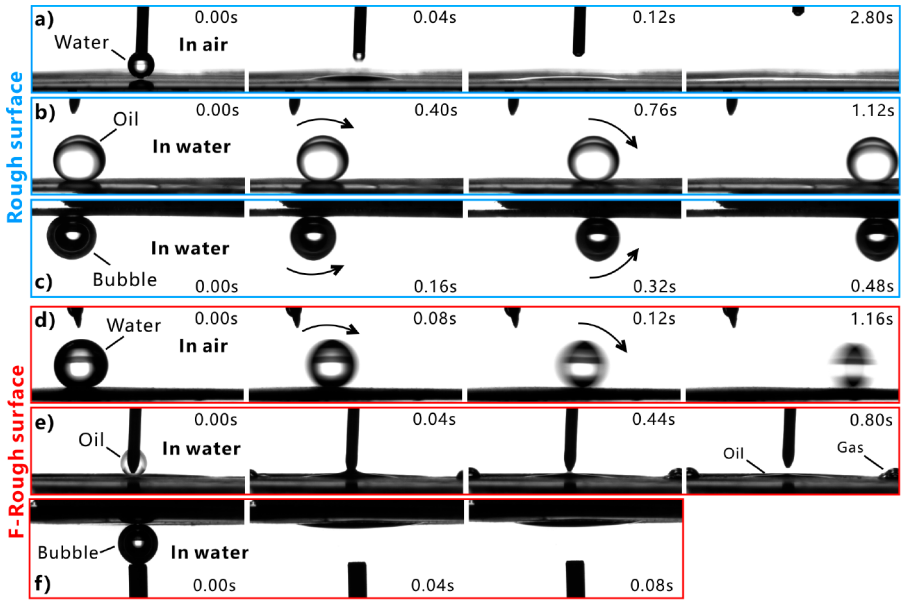

Figure 3. Dynamic wettability of the water droplet and the underwater oil droplet/bubble on the as-prepared surfaces. (a, e, f) Dispensing (a) a water droplet, (e) an oil droplet, and (f) an air bubble onto the resultant surface. (b, c, d) Processes of (b) an oil droplet, (c) an air bubble, and (d) a water droplet rolling off on the resultant surface. Substrates in (a−c) are the rough surfaces and those in (d−f) are the F-rough surfaces. The processes in (a, d) were performed in air, while the processes in (b, c, e, f) were performed in water.

DOI: 10.1021/acs.langmuir.8b03726
Langmuir 2019, 35, 921−927

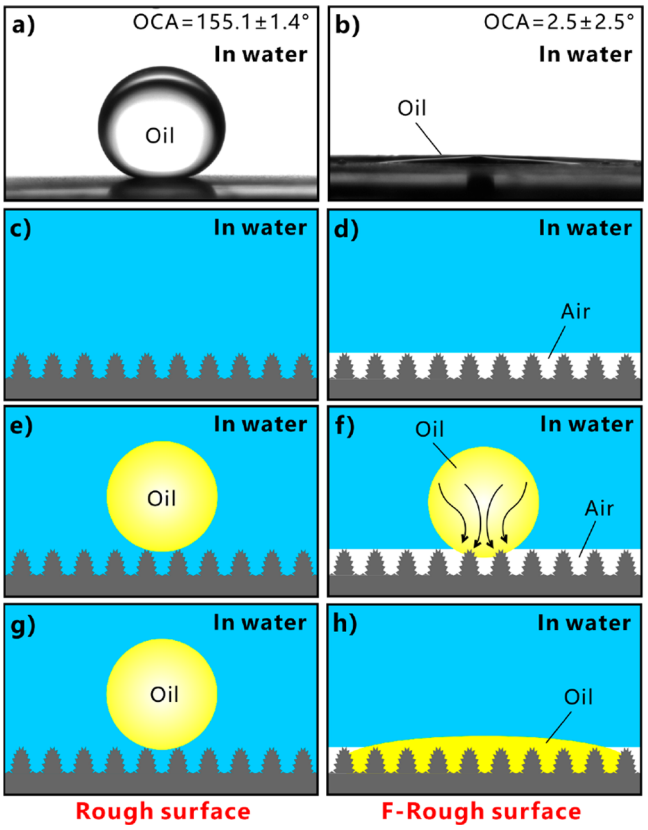

Figure 4. Underwater oil wettability of the rough and the F-rough surfaces, respectively. (a, b) Shapes of an oil droplet on (a) the rough surface and (b) the F-rough surface in water. (c, e, g) Forming principle of the underwater superoleophobicity of the laser-structured rough surface: (c) the rough microstructure in water, (e) placing an oil droplet onto the rough microstructure in water, and (g) after some time. (d, f, h) Forming principle of the underwater superoleophilicity of the F-rough microstructure: (d) the F-rough microstructure in water, (f) placing an oil droplet onto the F-rough microstructure in water, and (h) after some time.

the trapped water in the space between the surface microstructures. This trapped water provides a strong repulsive force to the oil droplet because of the repulsion between the polar and nonpolar molecules, preventing the oil from effectively touching the surface microstructures. The contact between such oil droplet and the rough surface is the underwater Cassie state.[1] After some time, the oil droplet keeps the sphere on the superhydrophilic surface in water (Figure 4g). The extremely small oil−Al contact area results in great underwater superoleophobicity of the original laser-structured surface. In contrast, if the oil droplet had been dripped onto the rough surface in air, the oil would have fully wet the microstructure. Most of the oil contaminants were able to be cleaned by water as the oil-wetted rough surface was dipped into water due to the superhydrophilicity of the rough microstructure.[46]

The F-rough surface shows a different oil-wettability from the rough surface in water. As the F-rough surface was immersed in water and then a small oil droplet was placed on this surface, the droplet spread out on the substrate after the two surfaces just touched each other (Figure 3e and Movie S4 in the Supporting Information). Finally, the oil droplet had a very small OCA of 2.5 ± 2.5° on the F-rough surface, demonstrating the underwater superoleophilicity of the F-rough surface (Figure 4b). Such a result agrees well with the underwater superoleophilicity of the fs laser-structured superhydrophobic Ti surface.[47] An ultrathin air layer forms between the surface microstructure and the surrounding water as the superhydrophobic surface is submerged in water (Figure 4d). The existence of this air layer is the direct result of the ultralow adhesive superhydrophobicity of the F-rough microstructure and is verified by the mirror-like reflectance (Figure 2f). When an oil droplet is moved into contact with this substrate, the droplet touches not only the top of the solid microstructures but also the trapped air layer (Figure 4f). Then the oil droplet enters into this thin air layer and is able to rapidly spread out along such an air layer under water pressure and the capillary effect (Figure 4f,h). As the oil occupies the spaces between the surface microstructure, gas is pushed outward and even out of the microstructure (see the last image in Figure 3e). As a result, the oil fully wets the F-rough microstructure, agreeing well with the underwater version of the Wenzel state (Figure 4h).[1]

Underwater Bubble Wettability. The behavior of an underwater bubble on the sample surface is very similar to that of an oil droplet. The rough surface showed superaerophobicity and ultralow adhesion to air bubbles in water. The bubble on the rough microstructure had a spherical shape with the bubble CA (BCA) of 154 ± 1° (Figure 5a). Once the sample was tilted to 0.5 ± 0.5°, the bubble easily rolled off (Figure 3c and Movie S5 in the Supporting Information). On the contrary, a small bubble spread out within 40 ms when the bubble was dispensed on the F-rough surface in water (Figure 3f and Movie S6 in the Supporting Information). Therefore, the F-rough surface exhibited underwater superaerophilicity with a BCA of 9.4 ± 3.6° to the bubbles (Figure 5b). Previously, we achieved underwater superaerophobicity and superaerophilicity on the fs laser-treated Si surface and the polydimethylsiloxane (PDMS) surface, respectively.[22]

The superhydrophilic rough surface is completely wetted by water in a water medium, even if the laser-treated side faces down (Figure 5c). If an air bubble is dispensed onto the rough surface in water, the bubble is repelled by the water trapped in the surface microstructure, as shown in Figure 5e. The strong repulsion is caused by the incompatibility between the water and the air. The efficient touch between the gas and the solid microstructure is prevented by this trapped water layer. Such an extremely small contact area does not increase after some time, allowing the bubble to be at the stable underwater Cassie state on the rough surface (Figure 5g). As a result, the laser-induced rough microstructure has underwater superaerophobicity. Regarding the ultralow adhesive superhydrophobic F-rough surface, a thin layer of air is formed on the textured area after immersion of the sample in water (Figure 2f and 5d). When an underwater bubble comes in contact with the F-rough surface, the gas in the bubble can easily enter into this trapped air layer, driven by the pressure of the water environment (Figure 5f). The bubble and the trapped air layer finally merge together. The bubble looks like it is being absorbed by the F-rough surface; thereby, such an F-rough surface shows underwater superaerophilicity (Figure 5h).

Relationship between the Different Superwettabilities. Different superwettabilities were obtained on the laser-structured Al surface, including superhydro-philicity/phobicity, underwater superoleophobicity/philicity, and underwater superaerophobicity/philicity. The original laser-induced hierarchical microstructures are superhydrophilic and have underwater superoleophobicity and superaerophobicity. On the

DOI: 10.1021/acs.langmuir.8b03726
Langmuir 2019, 35, 921−927

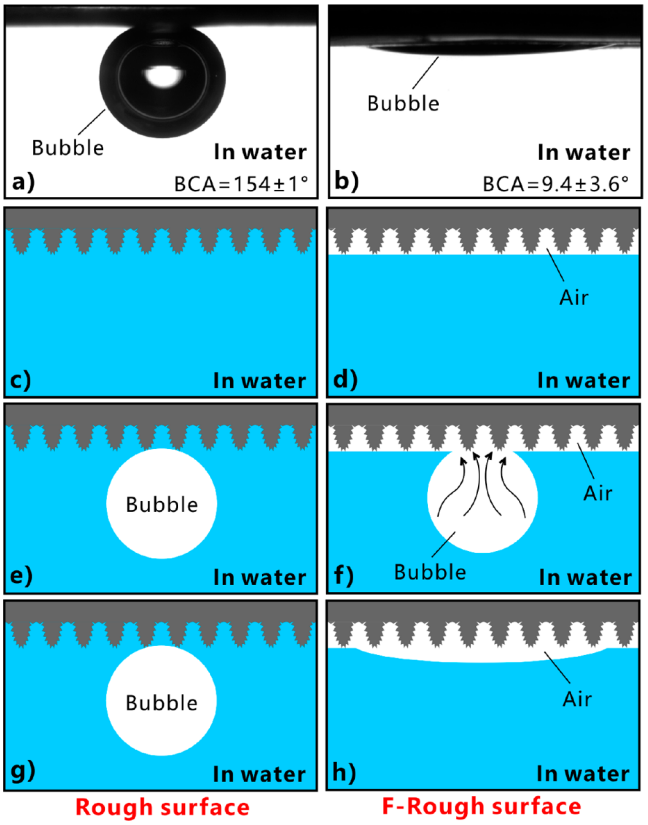

Figure 5. Underwater bubble wettability of the rough and the F-rough surfaces, respectively. (a, b) Images of a bubble on (a) the rough surface and (b) the F-rough surface in water. (c, e, g) Forming principle of the underwater superaerophobicity of the laser-structured rough surface: (c) the rough microstructure in water, (e) releasing an underwater bubble onto the rough microstructure, and (g) after some time. (d, f, h) Forming principle of the underwater superaerophilicity of the F-rough microstructure: (d) the F-rough microstructure in water, (f) releasing an underwater bubble onto the F-rough microstructure, and (h) after some time.

contrary, the fluoroalkylsilane-modified microstructures become superhydrophobic and exhibit superoleophilicity and superaerophilicity in water. The superhydrophilicity, superoleophilicity, and superaerophilicity of the material surfaces allow them to have the ability to absorb/capture/collect water, oil (underwater), and gas (underwater), whereas the surfaces with superhydrophobicity, superoleophobicity, and superaerophobicity have antiwater, antioil (underwater), and antibubble (underwater) functions, respectively.

It is demonstrated that the underwater oil/bubble wettabilities of a material surface are strongly associated with its water wettability. Figure 6 shows the relationship between the above-mentioned different superwettabilities. Hierarchical microstructures were simply built on the Al substrate by laser ablation (Figure 6a). The surface microstructure is able to amplify the wettability of the Al surface from intrinsic hydrophilicity to superhydrophilicity (Figure 6b). The contact between the in-air water droplet and the rough microstructure agrees well with the Wenzel state in which water fully wets the surface microstructure. If the sample is submerged in water, a water layer will be formed in the surface microstructure. At present, the oil droplet and bubble that are released onto the microstructure are at the underwater Cassie state. Therefore, the rough surface shows underwater superoleophobicity (Figure 6d) and superaerophobicity (Figure 6e). Fluoroalkylsilane modification is a common way to lower the surface energy of a solid substrate. After fluoroalkylsilane modification, the laser-induced microstructure turns to superhydrophobicity (Figure 6c). The water droplet only touches the peak of the F-rough microstructure and is at the Cassie state. A gas layer will be generated between the surface microstructures once the sample is dipped into water. At present, when an underwater small oil droplet or a bubble touches the F-rough structure, the oil/air in the droplet/bubble easily disperses along this thin air layer, resulting in an underwater Wenzel contact state at the interface of the oil droplet/bubble and the F-rough surface. As a result, the F-rough surface exhibits superoleophilicity (Figure 6f) and superaerophilicity (Figure 6g) in water.

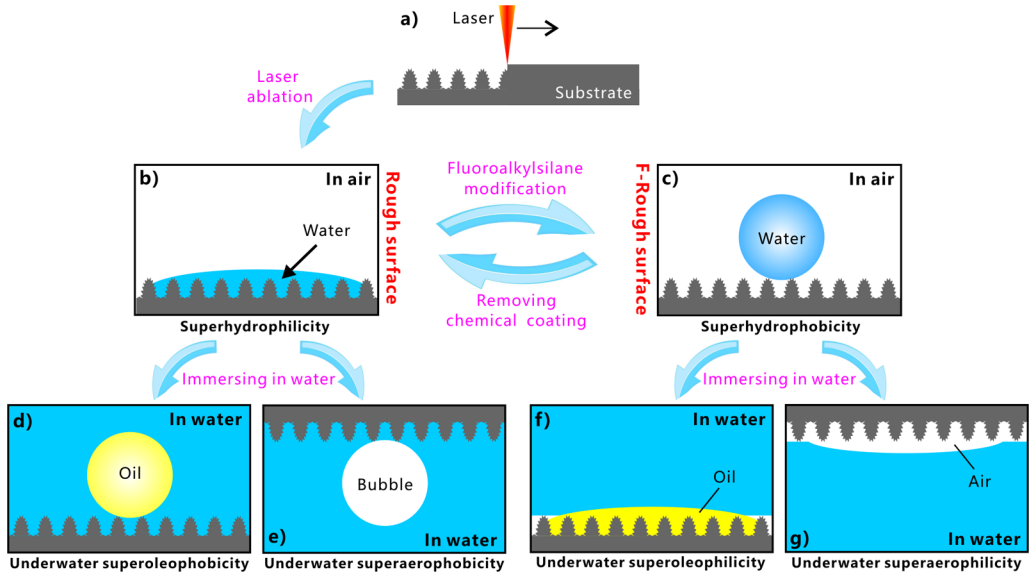

Figure 6. Relationship between different superwettabilities on the laser-ablated Al surface. (a) Generating surface microstructure by fs laser ablation. (b) Superhydrophilicity in air. (c) Superhydrophobicity in air. (d) Superoleophobicity in water. (e) Superaerophobicity in water. (f) Superoleophilicity in water. (g) Superaerophilicity in water.

DOI: 10.1021/acs.langmuir.8b03726
Langmuir 2019, 35, 921−927

Most superhydrophilic surfaces will show superoleophobicity and superaerophobicity after immersion in water, while most superhydrophobic surfaces with ultralow water adhesion will exhibit underwater superoleophilicity and superaerophilicity. The superhydrophilicity of the hierarchical microstructures can be switched to superhydrophobicity by chemical modification with a low-surface-energy monolayer (Figure 6c). The obtained superhydrophobicity can also get back to superhydrophilicity through the removal of the chemical coating (e.g., by slight oxygen plasma irradiation) or further chemical modification with a high-surface-energy monolayer (Figure 6b). Therefore, the obtained different superwettabilities can be transformed from and to each other.

Generally, superhydrophobic surfaces can always preserve their superhydrophobicity in air. In contrast, most superhydrophilic surfaces will gradually lose superhydrophilicity in air because such surfaces tend to absorb environmental carbon contaminants.[48] Fortunately, superhydrophilicity can be preserved for a very long time by storing the superhydrophilic surfaces in water. We find that the laser-induced rough surface has excellent superhydrophilicity, underwater superoleophobicity, and underwater superaerophobicity for more than one month as long as the sample is stored in water, while the laser-induced F-rough surface is able to always preserve superhydrophobicity, underwater superoleophilicity, and underwater superaerophilicity even the sample is stored in air.

CONCLUSIONS

In conclusion, different superwettabilities (including superhydrophilic, underwater superoleophobic, underwater superaerophobic, superhydrophobic, underwater superoleophilic, and underwater superaerophilic properties) were obtained on Al substrate with a fs laser-induced microstructured pattern. There is a close relationship between these superwettabilities, summarized from the experimental and theoretical analyses. The original laser-induced hierarchical microstructure is superhydrophilic, and it shows superoleophobicity/aerophobicity after immersion in water. When the microstructure is simply modified with fluoroalkylsilane, it switches to superhydrophobic properties in air. At present, the underwater superoleophilicity/aerophilicity are exhibited by the modified hierarchical microstructures. It is demonstrated that the underwater oil/bubble wettabilities of a solid surface are strongly influenced by its water wettability. The superhydrophilicity and the superhydrophobicity of the textured surface can be reversibly switched by the alternate low-surface-energy chemical modification and the removal of this coating. Hence, six states of superwettabilities can be realized on the same laser-treated substrate. The superhydrophilicity/oleophilicity/aerophilicity allow the sample surfaces to have the ability to absorb/capture water, oil, and gas, whereas the superhydrophobicity/oleophobicity/aerophobicity endow the sample surfaces with antiwater, antioil, and antibubble functions, respectively. The reported relationship between the above-mentioned superwettabilities has vital significance in the efficient design and preparation of different superwetting materials.

ASSOCIATED CONTENT

Supporting Information

The Supporting Information is available free of charge on the ACS Publications website at DOI: 10.1021/acs.langmuir.8b03726.

Process of dripping a water droplet onto the rough surface in air (Movie S1) (AVI)

Process of a water droplet rolling on the F-rough surface in air (Movie S2) (AVI)

Process of an oil droplet rolling on the rough surface in water (Movie S3) (AVI)

Process of dripping an oil droplet onto the F-rough surface in water (Movie S4) (AVI)

Process of an underwater bubble rolling on the rough surface (Movie S5) (AVI)

Process of an underwater bubble being absorbed by the F-rough surface (Movie S6) (AVI)

AUTHOR INFORMATION

Corresponding Authors

*E-mail: chenfeng@mail.xjtu.edu.cn.

*E-mail: guo@optics.rochester.edu.

ORCID

Feng Chen: 0000-0002-7031-7404

Chunlei Guo: 0000-0001-8525-6301

Notes

The authors declare no competing financial interest.

ACKNOWLEDGMENTS

This work is supported by the Bill & Melinda Gates Foundation under the Grant no. OPP1119542, National Key Research and Development Program of China under the Grant no. 2017YFB1104700, the National Science Foundation of China under the Grant nos. 51335008, 61875158, and 61805192, and the China Postdoctoral Science Foundation under the Grant no. 2016M600786.

REFERENCES

(1) Yong, J.; Chen, F.; Yang, Q.; Huo, J.; Hou, X. Superoleophobic Surfaces. *Chem. Soc. Rev.* **2017**, *46*, 4168−4217.

(2) Liu, X.; Liang, Y.; Zhou, F.; Liu, W. Extreme Wettability and Tunable Adhesion: Biomimicking Beyond Nature? *Soft Matter* **2012**, *8*, 2070−2086.

(3) Wang, M.; Chen, C.; Ma, J.; Xu, J. Preparation of Superhydrophobic Cauliflower-Like Silica Nanospheres with Tunable Water Adhesion. *J. Mater. Chem.* **2011**, *21*, 6962−6967.

(4) Yong, J.; Chen, F.; Yang, Q.; Zhang, D.; Du, G.; Si, J.; Yun, F.; Hou, X. Femtosecond Laser Weaving Superhydrophobic Patterned PDMS Surfaces with Tunable Adhesion. *J. Phys. Chem. C* **2013**, *117*, 24907−24912.

(5) Nishimoto, S.; Bhushan, B. Bioinspired Self-Cleaning Surfaces with Superhydrophobicity, Superoleophobicity, and Superhydrophilicity. *RSC Adv.* **2013**, *3*, 671−690.

(6) Ragesh, P.; Ganesh, V. A.; Nair, S. V.; Nair, A. S. A Review on 'Self-Cleaning and Multifunctional Materials'. *J. Mater. Chem. A* **2014**, *2*, 14773−14797.

(7) Xue, Z.; Cao, Y.; Liu, N.; Feng, L.; Jiang, L. Special Wettable Materials for Oil/Water Separation. *J. Mater. Chem. A* **2014**, *2*, 2445−2460.

(8) Wang, B.; Liang, W.; Guo, Z.; Liu, W. Biomimetic Super-Lyophobic and Super-Lyophilic Materials Applied for Oil/Water Separation: A New Strategy Beyond Nature. *Chem. Soc. Rev.* **2015**, *44*, 336−361.

(9) Yong, J.; Huo, J.; Chen, F.; Yang, Q.; Hou, X. Oil/Water Separation Based on Natural Materials with Super-Wettability: Recent Advances. *Phys. Chem. Chem. Phys.* **2018**, *20*, 25140−25163.

(10) Kreder, M. J.; Alvarenga, J.; Kim, P.; Aizenberg, J. Design of Anti-Icing Surfaces: Smooth, Textured or Slippery? *Nat. Rev. Mater.* **2016**, *1*, 1−15.

(11) Wang, S.; Wang, T.; Ge, P.; Xue, P.; Ye, S.; Chen, H.; Li, Z.; Zhang, J.; Yang, B. Controlling Flow Behavior of Water in Microfluidics with a Chemically Patterned Anisotropic Wetting Surface. *Langmuir* **2015**, *31*, 4032−4039.
(12) Songok, J.; Tuominen, M.; Teisala, H.; Haapanen, J.; Mäkelä, J.; Kuusipalo, J.; Toivakka, M. Paper-Based Microfluidics: Fabrication Technique and Dynamics of Capillary-Driven Surface Flow. *ACS Appl. Mater. Interfaces* **2014**, *6*, 20060−20066.
(13) Stratakis, E.; Ranella, A.; Fotakis, C. Biomimetic Micro/Nanostructured Functional Surfaces for Microfluidic and Tissue Engineering Applications. *Biomicrofluidics* **2011**, *5*, 013411.
(14) Ranella, A.; Barberoglou, M.; Bakogianni, S.; Fotakis, C.; Stratakis, E. Tuning Cell Adhesion by Controlling the Roughness and Wettability of 3D Micro/Nano Silicon Structure. *Acta Biomater.* **2010**, *6*, 2711−2720.
(15) Shen, L.; Wang, B.; Wang, J.; Fu, J.; Picart, C.; Ji, J. Asymmetric Free-Standing Film with Multifunctional Anti-Bacterial and Self-Cleaning Properties. *ACS Appl. Mater. Interfaces* **2012**, *4*, 4476−4483.
(16) Zhang, S.; Huang, J.; Chen, Z.; Lai, Y. Bioinspired Special Wettability Surfaces: From Fundamental Research to Water Harvesting Applications. *Small* **2017**, *13*, 1602992.
(17) Gupta, R., K.; Dunderdale, G. J.; England, M. W.; Hozumi, A. Oil/Water Separation Techniques: A Review of Recent Progress and Future Directions. *J. Mater. Chem. A* **2017**, *5*, 16025−16058.
(18) Yong, J.; Chen, F.; Huo, J.; Fang, Y.; Yang, Q.; Zhang, J.; Hou, X. Femtosecond Laser Induced Underwater Superaerophilic and Superaerophobic PDMS Sheets with Through Microholes for Selective Passage of Air Bubble and Further Collection of Underwater Gas. *Nanoscale* **2018**, *10*, 3688−3696.
(19) Barthlott, W.; Neinhuis, C. Purity of the Sacred Lotus, or Escape from Contamination in Biological Surfaces. *Planta* **1997**, *202*, 1−8.
(20) Feng, L.; Li, S.; Li, Y.; Li, H.; Zhang, L.; Zhai, J.; Song, Y.; Liu, B.; Jiang, L.; Zhu, D. Super-Hydrophobic Surfaces: From Natural to Artificial. *Adv. Mater.* **2002**, *14*, 1857−1860.
(21) Zorba, V.; Stratakis, E.; Barberoglou, M.; Spanakis, E.; Tzanetakis, P.; Anastasiadis, S. H.; Fostas, C. Biomimetic Artificial Surfaces Quantitatively Reproduce the Water Repellency of a Lotus Leaf. *Adv. Mater.* **2008**, *20*, 4049−4054.
(22) Yong, J.; Chen, F.; Fang, Y.; Huo, J.; Yang, Q.; Zhang, J.; Bian, H.; Hou, X. Bioinspired Design of Underwater Superaerophobic and Superaerophilic Surfaces by Femtosecond Laser Ablation for Anti- or Capturing Bubbles. *ACS Appl. Mater. Interfaces* **2017**, *9*, 39863−39871.
(23) Liu, M.; Wang, S.; Wei, Z.; Song, Y.; Jiang, L. Bioinspired Design of a Superoleophobic and Low Adhesive Water/Solid Interface. *Adv. Mater.* **2009**, *21*, 665−669.
(24) Yong, J.; Chen, F.; Li, M.; Yang, Q.; Fang, Y.; Huo, J.; Hou, X. Remarkably Simple Achievement of Superhydrophobicity, Superhydrophilicity, Underwater Superoleophobicity, Underwater Superoleophilicity, Underwater Superaerophobicity, and Underwater Superaerophilicity on Femtosecond Laser Ablated PDMS Surfaces. *J. Mater. Chem. A* **2017**, *5*, 25249−25257.
(25) Tian, Y.; Su, B.; Jiang, L. Interfacial Material System Exhibiting Superwettability. *Adv. Mater.* **2014**, *26*, 6872−6897.
(26) Wen, L.; Tian, Y.; Jiang, L. Bioinspired Super-Wettability from Fundamental Research to Practical Applications. *Angew. Chem., Int. Ed.* **2015**, *54*, 3387−3399.
(27) Liu, M.; Wang, S.; Jiang, L. Nature-Inspired Superwettability Systems. *Nat. Rev. Mater.* **2017**, *2*, 17036.
(28) Su, B.; Tian, Y.; Jiang, L. Bioinspired Interfaces with Superwettability: From Materials to Chemistry. *J. Am. Chem. Soc.* **2016**, *138*, 1727−1748.
(29) Bellanger, H.; Darmanin, T.; Taffin de Givenchy, E.; Guittard, F. Chemical and Physical Pathways for the Preparation of Superoleophobic Surfaces and Related Wetting Theories. *Chem. Rev.* **2014**, *114*, 2694−2716.
(30) Wang, J.-N.; Zhang, Y.-L.; Liu, Y.; Zheng, W.; Lee, L. P.; Sun, H.-B. Recent Developments in Superhydrophobic Graphene and Graphene-Related Materials: From Preparation to Potential Applications. *Nanoscale* **2015**, *7*, 7101−7114.
(31) Yong, J.; Chen, F.; Yang, Q.; Hou, X. Femtosecond Laser Controlled Wettability of Solid Surface. *Soft Matter* **2015**, *11*, 8897−8906.
(32) Wu, B.; Zhou, M.; Li, J.; Ye, X.; Li, G.; Cai, L. Superhydrophobic Surfaces Fabricated by Microstructuring of Stainless Steel Using a Femtosecond Laser. *Appl. Surf. Sci.* **2009**, *256*, 61−66.
(33) Vorobyev, A. Y.; Guo, C. Multifunctional Surfaces Produced by Femtosecond Laser Pulses. *J. Appl. Phys.* **2015**, *117*, 033103.
(34) Vorobyev, A. V.; Guo, C. Metal Pumps Liquid Uphill. *Appl. Phys. Lett.* **2009**, *94*, 224102.
(35) Vorobyev, A. V. Guo, Laser Turns Silicon Superwicking. C. *Opt. Express* **2010**, *18*, 6455.
(36) Vorobyev, A. V.; Guo, C. Water Sprints Uphill on Glass. *J. Appl. Phys.* **2010**, *108*, 123512.
(37) Vorobyev, A. V.; Guo, C. Making Human Enamel and Dentin Surfaces Superwetting for Enhanced Adhesion. *Appl. Phys. Lett.* **2011**, *99*, 193703.
(38) Baldacchini, T.; Carey, J. E.; Zhou, M.; Mazur, E. Superhydrophobic Surfaces Prepared by Microstructuring of Silicon Using a Femtosecond Laser. *Langmuir* **2006**, *22*, 4917−4919.
(39) Yong, J.; Yang, Q.; Chen, F.; Zhang, D.; Bian, H.; Ou, Y.; Si, J.; Du, G.; Hou, X. Stable Superhydrophobic Surface with Hierarchical Mesh-Porous Structure Fabricated by a Femtosecond Laser. *Appl. Phys. A: Mater. Sci. Process.* **2013**, *111*, 243−249.
(40) Yong, J.; Yang, Q.; Chen, F.; Zhang, D.; Farooq, U.; Du, G.; Hou, X. A Simple Way to Achieve Superhydrophobicity, Controllable Water Adhesion, Anisotropic Sliding, and Anisotropic Wetting Based on Femtosecond-Laser-Induced Line-Patterned Surfaces. *J. Mater. Chem. A* **2014**, *2*, 5499−5507.
(41) Yong, J.; Fang, Y.; Chen, F.; Huo, J.; Yang, Q.; Bian, H.; Du, G.; Hou, X. Femtosecond Laser Ablated Durable Superhydrophobic PTFE Films with Micro-Through-Holes for Oil/Water Separation: Separating Oil from Water and Corrosive Solutions. *Appl. Surf. Sci.* **2016**, *389*, 1148−1155.
(42) Yong, J.; Chen, F.; Yang, Q.; Fang, Y.; Huo, J.; Hou, X. Femtosecond Laser Induced Hierarchical ZnO Superhydrophobic Surfaces with Switchable Wettability. *Chem. Commun.* **2015**, *51*, 9813−9816.
(43) Zhao, Y.; Tang, Y.; Wang, X.; Lin, T. Superhydrophobic Cotton Fabric Fabricated by Electrostatic Assembly of Silica Nanoparticles and Its Remarkable Buoyancy. *Appl. Surf. Sci.* **2010**, *256*, 6736−6742.
(44) Larmour, I. A.; Bell, S. E. J.; Saunders, G. C. Remarkably Simple Fabrication of Superhydrophobic Surfaces Using Electroless Galvanic Deposition. *Angew. Chem. Int. Ed.* **2007**, *46*, 1710−1712.
(45) Li, G.; Fan, H.; Ren, F.; Zhou, C.; Zhang, Z.; Xu, B.; Wu, S.; Hu, Y.; Zhu, W.; Zeng, Y.; Li, X.; Chu, J.; Wu, D. Multifunctional Ultrathin Aluminum Foil: Oil/Water Separation and Particle Filtration. *J. Mater. Chem. A* **2016**, *4*, 18832−18840.
(46) Wu, D.; Wu, S.-Z.; Chen, Q.-D.; Zhao, S.; Zhang, H.; Jiao, J.; Piersol, J. A.; Wang, J.-N.; Sun, H.-B.; Jiang, L. Facile Creation of Hierarchical PDMS Microstructures with Extreme Underwater Superoleophobicity for Anti-Oil Application in Microfluidic Channels. *Lab Chip* **2011**, *11*, 3873−3879.
(47) Yong, J.; Chen, F.; Yang, Q.; Farooq, U.; Hou, X. Photoinduced Switchable Underwater Superoleophobicity-Superoleophilicity on Laser Modified Titanium Surfaces. *J. Mater. Chem. A* **2015**, *3*, 10703−10709.
(48) Yan, H.; Rashid, M. R. B. A.; Khew, S. Y.; Li, F.; Hong, M. Wettability Transition of Laser Textured Brass Surfaces Inside Different Mediums. *Appl. Surf. Sci.* **2018**, *427*, 369−375.

DOI: 10.1021/acs.langmuir.8b03726
Langmuir 2019, 35, 921−927